

Short-range surface plasmon propagation supported by stimulated amplification using electrical injection

Yicen Li,¹ Hui Zhang,² Ning Zhu,² Ting Mei,^{2,*} Dao Hua Zhang,¹ and Jinghua Teng³

¹Nanophotonics Laboratory, School of Electrical and Electronic Engineering, Nanyang Technological University, Singapore 639798, Singapore

²Institute of Optoelectronic Materials and Technology, South China Normal University, Guangzhou 510631, China

³Institute of Material Research and Engineering, Singapore 117602, Singapore

*ting.mei@ieee.org

Abstract: We have investigated the propagation of the long-range mode (LRSP) and the short-range mode (SRSP) surface plasmon polaritons (SPPs) along the waveguide made from Au film and quantum wells (QWs) gain medium. Influenced by the gain spectral nonuniformity, the SRSP showed narrower spectrum than the LRSP in output, denoting that the SRSP propagation was supported by stimulated amplification (SA) in electrically-pumped QWs. An SRSP output power as large as 1.6 times of that of the LRSP was obtained over a travelling distance of 80 μ m. The mechanism of SA-supported SRSP propagation can be adopted for electrical modulation of SPPs.

©2011 Optical Society of America

OCIS codes: (240.6680) Surface plasmons; (250.5590) Quantum-well, -wire and -dot devices; (250.5403) Plasmonics.

References and links

1. S. A. Maier and H. A. Atwater, "Plasmonics: Localization and guiding of electromagnetic energy in metal/dielectric structures," *J. Appl. Phys.* **98**(1), 011101 (2005).
2. J. A. Schuller, E. S. Barnard, W. S. Cai, Y. C. Jun, J. S. White, and M. L. Brongersma, "Plasmonics for extreme light concentration and manipulation," *Nat. Mater.* **9**(3), 193–204 (2010).
3. D. K. Gramotnev and S. I. Bozhevolnyi, "Plasmonics beyond the diffraction limit," *Nat. Photonics* **4**(2), 83–91 (2010).
4. D. J. Bergman and M. I. Stockman, "Surface plasmon amplification by stimulated emission of radiation: quantum generation of coherent surface plasmons in nanosystems," *Phys. Rev. Lett.* **90**(2), 027402 (2003).
5. M. A. Noginov, G. Zhu, M. Mayy, B. A. Ritzo, N. Noginova, and V. A. Podolskiy, "Stimulated emission of surface plasmon polaritons," *Phys. Rev. Lett.* **101**(22), 226806 (2008).
6. M. A. Noginov, V. A. Podolskiy, G. Zhu, M. Mayy, M. Bahoura, J. A. Adegoke, B. A. Ritzo, and K. Reynolds, "Compensation of loss in propagating surface plasmon polariton by gain in adjacent dielectric medium," *Opt. Express* **16**(2), 1385–1392 (2008).
7. J. Grandidier, G. C. des Francs, S. Massenet, A. Bouhelier, L. Markey, J. C. Weeber, C. Finot, and A. Dereux, "Gain-assisted propagation in a plasmonic waveguide at telecom wavelength," *Nano Lett.* **9**(8), 2935–2939 (2009).
8. I. P. Radko, M. G. Nielsen, O. Albrektsen, and S. I. Bozhevolnyi, "Stimulated emission of surface plasmon polaritons by lead-sulphide quantum dots at near infra-red wavelengths," *Opt. Express* **18**(18), 18633–18641 (2010).
9. G. Colas des Francs, P. Bramant, J. Grandidier, A. Bouhelier, J. C. Weeber, and A. Dereux, "Optical gain, spontaneous and stimulated emission of surface plasmon polaritons in confined plasmonic waveguide," *Opt. Express* **18**(16), 16327–16334 (2010).
10. P. M. Bolger, W. Dickson, A. V. Krasavin, L. Liescher, S. G. Hickey, D. V. Skryabin, and A. V. Zayats, "Amplified spontaneous emission of surface plasmon polaritons and limitations on the increase of their propagation length," *Opt. Lett.* **35**(8), 1197–1199 (2010).
11. D. Yu. Fedyanin and A. V. Arsenin, "Surface plasmon polariton amplification in metal-semiconductor structures," *Opt. Express* **19**(13), 12524–12531 (2011).
12. R. F. Oulton, V. J. Sorger, T. Zentgraf, R. M. Ma, C. Gladden, L. Dai, G. Bartal, and X. Zhang, "Plasmon lasers at deep subwavelength scale," *Nature* **461**(7264), 629–632 (2009).

13. Z. J. Yang, N. C. Kim, J. B. Li, M. T. Cheng, S. D. Liu, Z. H. Hao, and Q. Q. Wang, "Surface plasmons amplifications in single Ag nanoring," *Opt. Express* **18**(5), 4006–4011 (2010).
14. M. T. Hill, M. Marell, E. S. P. Leong, B. Smalbrugge, Y. C. Zhu, M. H. Sun, P. J. van Veldhoven, E. J. Geluk, F. Karouta, Y. S. Oei, R. Notzel, C. Z. Ning, and M. K. Smit, "Lasing in metal-insulator-metal sub-wavelength plasmonic waveguides," *Opt. Express* **17**(13), 11107–11112 (2009).
15. A. Babuty, A. Bousseksou, J. P. Tetienne, I. M. Doyen, C. Sirtori, G. Beaudoin, I. Sagnes, Y. De Wilde, and R. Colombelli, "Semiconductor surface plasmon sources," *Phys. Rev. Lett.* **104**(22), 226806 (2010).
16. P. Neutens, L. Lagae, G. Borghs, and P. Van Dorpe, "Electrical excitation of confined surface plasmon polaritons in metallic slot waveguides," *Nano Lett.* **10**(4), 1429–1432 (2010).
17. S. A. Maier, "Gain-assisted propagation of electromagnetic energy in subwavelength surface plasmon polariton gap waveguides," *Opt. Commun.* **258**(2), 295–299 (2006).
18. D. B. Li and C. Z. Ning, "Giant modal gain, amplified surface plasmon-polariton propagation, and slowing down of energy velocity in a metal-semiconductor-metal structure," *Phys. Rev. B* **80**(15), 153304 (2009).
19. J. J. Burke, G. I. Stegeman, and T. Tamir, "Surface-polariton-like waves guided by thin, lossy metal films," *Phys. Rev. B Condens. Matter* **33**(8), 5186–5201 (1986).
20. L. Wendler and R. Haupt, "Long-range surface plasmon-polaritons in asymmetric layer structures," *J. Appl. Phys.* **59**(9), 3289–3291 (1986).
21. M. P. Nezhad, K. Tetz, and Y. Fainman, "Gain assisted propagation of surface plasmon polaritons on planar metallic waveguides," *Opt. Express* **12**(17), 4072–4079 (2004).
22. M. Z. Alam, J. Meier, J. S. Aitchison, and M. Mojahedi, "Gain assisted surface plasmon polariton in quantum wells structures," *Opt. Express* **15**(1), 176–182 (2007).
23. X. J. Zhang, Y. C. Li, T. Li, S. Y. Lee, C. G. Feng, L. B. Wang, and T. Mei, "Gain-assisted propagation of surface plasmon polaritons via electrically pumped quantum wells," *Opt. Lett.* **35**(18), 3075–3077 (2010).
24. J. Chilwell and I. Hodgkinson, "Thin-films field-transfer matrix theory of planar multilayer waveguides and reflection from prism-loaded waveguides," *J. Opt. Soc. Am. A* **1**(7), 742–753 (1984).
25. C. K. Chen, P. Berini, D. Z. Feng, S. Tanev, and V. P. Tzolov, "Efficient and accurate numerical analysis of multilayer planar optical waveguides in lossy anisotropic media," *Opt. Express* **7**(8), 260–272 (2000).
26. B. Broberg and S. Lindgren, "Refractive-index of $\text{In}_{1-x}\text{Ga}_x\text{As}_y\text{P}_{1-y}$ layers and InP in the transparent wavelength region," *J. Appl. Phys.* **55**(9), 3376–3381 (1984).
27. J. Minch, S. H. Park, T. Keating, and S. L. Chuang, "Theory and experiment of $\text{In}_{1-x}\text{Ga}_x\text{As}_y\text{P}_{1-y}$ and $\text{In}_{1-x-y}\text{Ga}_x\text{Al}_y\text{As}$ long-wavelength strained quantum-well lasers," *IEEE J. Quantum Electron.* **35**(5), 771–782 (1999).
28. D. Pacifici, H. J. Lezec, and H. A. Atwater, "All-optical modulation by plasmonic excitation of CdSe quantum dots," *Nat. Photonics* **1**(7), 402–406 (2007).
29. A. V. Krasavin, T. P. Vo, W. Dickson, P. M. Bolger, and A. V. Zayats, "All-plasmonic modulation via stimulated emission of copropagating surface plasmon polaritons on a substrate with gain," *Nano Lett.* **11**(6), 2231–2235 (2011).

1. Introduction

Surface plasmon polaritons (SPPs), as quanta of collective oscillations of free-electron gas coupling with the electromagnetic field at the metal/dielectric interface, are very sensitive to the optical properties of the supporting materials. Nowadays great interest is being paid to the interaction between active media and SPPs, for manipulating light over sub-wavelength dimensions [1–3]. In practical application, however, SPP propagation is always limited by its intrinsic loss due to metal absorption. Hence, fundamental study on loss compensation and even amplification of SPPs has become a topic which inspires much enthusiastic research [4–11]. Comparing with other gain materials, semiconductors with low-dimensional structures, i.e., quantum wells (QWs), quantum wires, and quantum dots, exhibit appealing capabilities on interacting with SPPs, benefiting from engineering on the electronic density of states and gain properties of the materials. Recently, SPP sources and lasers have been experimentally demonstrated using these materials, by either optical or electrical pumping [12–16]. The active SPP devices based on these high-gain materials are highly promising for bio-sensing, photonic integrated circuits and optical communications in the near future.

The interaction of the gain medium and SPPs depends largely on the coupling strength between the evanescent electromagnetic field and the excited electron-hole pairs in the active region. This demands that the active region should be located as close as possible to the interface if no resonant structure is employed for field enhancement [17, 18]. The long-range mode SPPs (LRSPs) and short-range mode SPPs (SRSPs) are supported in an asymmetric SPP guide structure with a thin metal film sandwiched between two dielectrics of high refractive index contrast [19, 20], which, for instance, can be implemented simply by

depositing a thin metal film on a semiconductor gain medium. Such a configuration with semiconductor gain materials, or more specifically QWs, has been investigated theoretically [21, 22] and experimentally [23] for gain-assisted SPPs.

In our previous work [23], we have demonstrated the manipulation of SPP propagation with electrical-pumping QWs located within the range of the SPP field, accompanied with hypothetical explanation based on numerical simulation. In this work, we conducted experimental investigation to further understand the mechanism of SPP propagations. Spectral characteristics and responses to the input and bias have been studied, while results and discussion are presented in the article.

2. Device fabrication and measurement experiment

The same material structure as that used in Ref [23]. was employed in this study, which contained three InGaAsP quantum wells (QWs) grown on n^+ -InP substrate by metal-organic chemical vapor deposition (MOCVD), as shown in Fig. 1(a). The QWs were designed with tensile strain to maximize TM gain near the telecom wavelength $1.55\mu\text{m}$. A groove window was wet-etched down to expose Layer #6, on top of which a 40nm-thick Au film was deposited and the SPP waveguide was fabricated. The etching process was strictly controlled to prepare a clean and uniform surface 40nm above the QW layers for the successive Au film deposition. The metal contact was made on the top p^+ -InGaAs contact layer to provide lateral current injection to the metal waveguide region, and the electrical contact pad was made on top of the Si_3N_4 insulating film. Electron beam lithography and lift-off processes were adopted to create the metal gratings and the SPP waveguide shown in Fig. 1(b). The total area under electrical injection is $8000\mu\text{m}^2$ while the waveguide is $80\mu\text{m}$ long and $25\mu\text{m}$ wide, giving an area of $2000\mu\text{m}^2$. Considering the serial resistance in the lateral injection, it is estimated that only 1/200 of the total current was directly injected to the waveguide area.

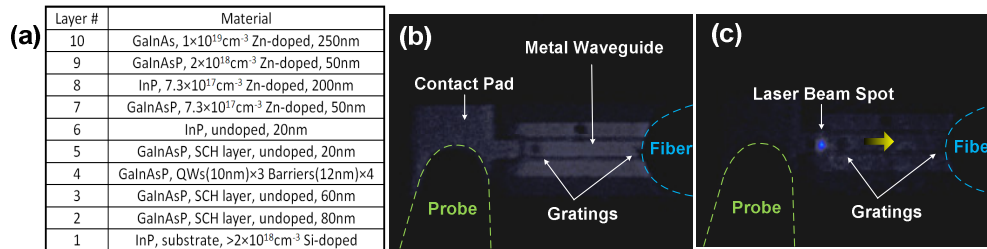


Fig. 1. (a) The epitaxial structure with InGaAsP multiple QWs grown on n^+ -InP substrate. (b) Device under test. In- and out- coupling gratings are fabricated on the ends of the metal waveguide. The electrical probe and the fiber probe are indicated. (c) The laser beam is focused on the in-coupling grating to excite SPPs in the metal waveguide.

In the experiment, a laser beam at the telecom wavelength was focused on the in-coupling grating through a $10\times$ long working distance objective lens. The spot size was controlled to be less than $5\mu\text{m}$ in diameter. SPPs were excited on the grating, propagated along the waveguide, and decoupled at another grating to free-space light collected by a fiber probe as shown in Fig. 1(c). Signals were collected by lock-in detection in two configurations: (i) input chopping, i.e. chopping the laser beam before coupling into the waveguide, and (ii) output chopping, i.e. chopping the collected output light. The measured results under various sets of conditions are shown in Fig. 2. In input-chopping measurements, i.e., in Fig. 2(a)-(c), the spectra showed sharp spikes in response to the input light, and the spectrum shapes resembled to that of the input laser. In output-chopping measurements, i.e., in Fig. 2(d)-(f), spontaneous emission (SE) was included, showing a widespread spectrum. The SE spectra have identical shapes under different biases and are irrelevant to the spectral spikes which respond to the input. This implies that the received SE component was essentially from the out-coupling grating area rather than the waveguide.

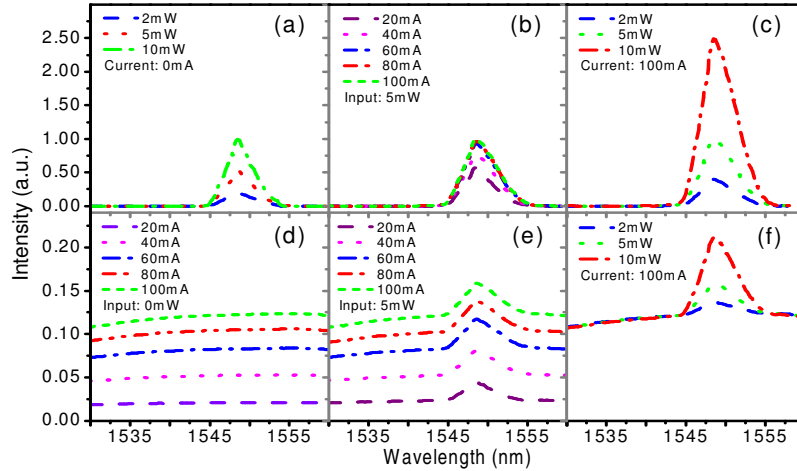


Fig. 2. (a)–(c) Spectra measured under the input-chopping configuration; (d)–(f) Spectra measured under the output-chopping configuration.

3. Numerical analysis of LRSP and SRSP propagation

Analysis using the transfer matrix method (TMM) and Cauchy integration method (CIM) [24, 25] shows that the multilayer structure supports only two TM bound modes, i.e., LRSP and SRSP. The refractive indices of all layers are obtained from Ref [26]. and the mode solutions are solved under transparency condition, i.e. without gain or loss. Their propagation lengths are influenced differently by the QW gain as seen in Fig. 3(a), and the two modes propagate independently of each other. The latter is illustrate in Fig. 3(b), where we assume a joint waveguide with a gain section and a transparent section end-fire coupled by a Gaussian beam to excite a field combining SRSP and LRSP modes. The two modes can be clearly identified from the two peaks in the intensity profiles. With sufficiently large gain, e.g., $\text{Im}(n_{\text{eff}})=0.1i$, in reference to Fig. 3(a), the SRSP mode localized on the QW side is amplified in the gain section, but decays rapidly in the transparent section. The propagation of the LRSP mode distributed on the air side, on the other hand, is hardly affected by the gain in QWs. Therefore, the LRSP and SRSP propagations are uncoupled and separable in data analysis.

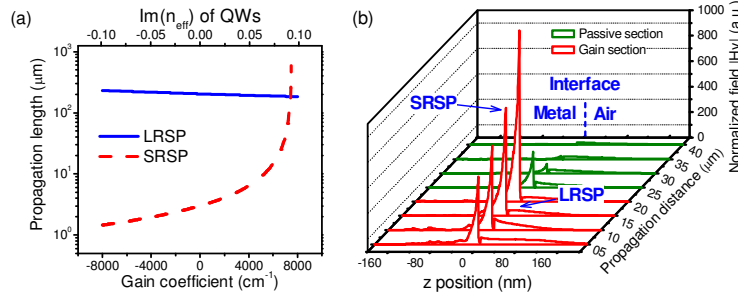


Fig. 3. (a) The calculated propagation length dependence on the QW gain coefficient for both LRSP and SRSP. (b) The calculated SPP field profiles along the propagation distance. The SPP fields are end-fire coupled into the gain section (red curves) using a Gaussian source and then travel into the transparent passive waveguide.

4. Spectrum analysis

In the input-chopping and output-chopping measurements, the signal formations can be written as

$$S_{IC}(\lambda; P, I) = c_{LRSP}(\lambda; P, I) f_{LRSP}(\lambda) + c_{SRSP}(\lambda; P, I) f_{SRSP}(\lambda), \text{ and}$$

$S_{OC}(\lambda; P, I) = c_{LRSP}(\lambda; P, I)f_{LRSP}(\lambda) + c_{SRSP}(\lambda; P, I)f_{SRSP}(\lambda) + c_{SE}(\lambda; P, I)f_{SE}(\lambda)$, respectively, where $f(\lambda)$ denotes the spectral shape function normalized at the input peak wavelength $\lambda_0 = 1.55\mu\text{m}$ and $c(\lambda; P, I)$ represents the weight factor of each component at the input power P and the bias current I . $f_{SE}(\lambda)$ was obtained from the data measured in output-chopping configuration at zero input given in Fig. 2(d). $f_{LRSP}(\lambda)$ was obtained from the data measured in the input-chopping configuration under zero bias given in Fig. 2(a). The spectral curves were normalized at the peak wavelength and then averaged to derive the spectral functions in order to ensure good accuracy. $f_{SRSP}(\lambda)$ was obtained from the differences of the data under no bias [Fig. 2(a)] and under bias [Fig. 2(c)] with the same averaging procedure performed. These spectral shape functions are plotted in Fig. 4(a) and there is a difference between $f_{LRSP}(\lambda)$ and $f_{SRSP}(\lambda)$, implying different propagation mechanisms of these two SPP modes.

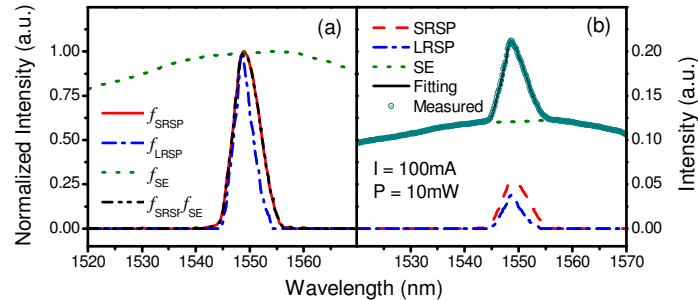


Fig. 4. (a) Normalized spectral shape functions for SRPP, LRSP, SE and the product of the SRSP and SE's spectral shape functions. (b) Three-peak curve fitting for the spectrum measured under 10mW laser input and 100mA current injection.

Supposing that the SRSP mode propagation is supported by stimulated amplification (SA), the spectrum of the SRSP output would be determined by the product of the input spectrum and the gain spectrum. The received LRSP output was the direct transmission of the input through the SPP waveguide and thus had the same spectrum as that of the input, whereas the gain spectrum is related to the SE spectrum as [27], $g(\omega) = g_{sp}(\omega)\{1 - \exp[(\hbar\omega - \Delta F)/k_B T]\} \propto g_{sp}(\omega)$, where ΔF is the quasi-Fermi level separation and $g_{sp}(\omega)$ is the spontaneous emission coefficient. Therefore, there should be such a spectral shape function relation as $f_{SRSP}(\lambda) = f_{LRSP}(\lambda) \cdot f_{SE}(\lambda)$. Verification of this relation is nicely done in Fig. 4(a) and can be regarded as the experimental evidence of SA-supported SRSP propagation.

These spectral shape functions were adopted for curve fitting the output-chopping measurement. An example is given in Fig. 4(b) showing good agreement between the fitting curve and the experimental data.

5. Variation trends

By curve-fitting the data of the output-chopping measurement using the three spectral shape functions, their respective weight factors were obtained. Figure 5 shows the variation trends of these components for varying input power or the bias current. The LRSP component was independent of the current bias but arose linearly with increasing input power as illustrated in Fig. 5(a)&(d), since the gain has minimal effect on LRSP. The SE component arose linearly with increasing bias current, but was not affected by the input power. In another word, the SE-SA competition [10] was not obviously observed and we suspected that SE from the out-coupling grating area might contribute to the output signal dominantly. There is apparent saturation due to high current injection as shown in Fig. 5(b) and corresponding in Fig. 2, but not due to high input power as shown in Fig. 5(e). At high current injection, carrier leakage, i.e. carriers passing through the active region without being captured by QWs, may increase due to the quasi-Fermi level rise and device temperature rise, causing the saturation in output.

Under the experimental condition, the SRSP component has achieved 1.6 times of the LRSP component in output power after travelling over a distance of $80\mu\text{m}$ with the SA support.

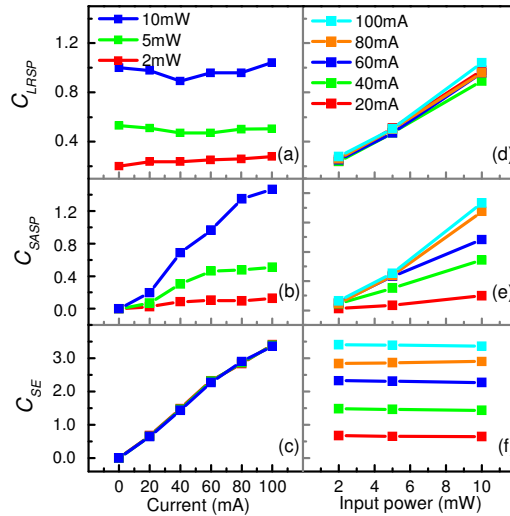


Fig. 5. The weight factors against the current injection and laser input intensity obtained from spectrum fitting. The left column (a~c) shows the plots with varying bias current. The right column (d~f) shows the plots with varying laser power.

In both Fig. 5(b)&(e), it is seen that this device has perfect control on SRSP propagation via SA. SRSPs were rejected in the output under zero bias, while leveled up beyond that of LRSPs under the current bias. This mechanism gives benefits of not only loss compensation, but also high on/off ratio to the electrical control of SPPs, alternative to the optical control of SPPs [28, 29]. To achieve high on/off ratio, modifications such as increasing the metal thickness and superstrate refractive index can be easily done for LRSP suppression. More aspects of optimization on optical and geometrical parameters for lossless SPP propagation have been introduced by Alam, et al in Ref [22].

6. Conclusion

We have experimentally investigated a series of output spectra under varying input power and bias current in the input-chopping and output-chopping configurations for an SPP waveguide on an electrical-pumping QW gain medium. Spectral shape functions of LRSP, SRSP and SE were derived from these spectra, and their weights were estimated, which have evidenced that the SRSP mode propagation was supported by SA. In our experimental observation, the SRSP component has achieved 1.6 times of the LRSP component in output power after travelling over a distance of $80\mu\text{m}$. The mechanism of SA-supported SRSP propagation can be employed for high-on/off-ratio and low-loss electrical SPPs modulation, for which the LRSP mode needs to be minimized in possible engineering approaches.

Acknowledgments

This work was financially supported by the Singapore National Research Foundation (CRP Award No. NRF-G-CRP 2007-01). T. Mei acknowledges support from Department of Education of Guangdong Province, China (Grant No. C10131).